ELSEVIER

Journal of Biomechanics 41 (2008) 430–437

JOURNAL OF BIOMECHANICS

www.elsevier.com/locate/jbiomech
www.JBiomech.com

Transport of neutral solute in articular cartilage: Effect of microstructure anisotropy

Le Zhang, Andras Z. Szeri*

Department of Mechanical Engineering, Center for Biomedical Engineering Research, University of Delaware, Newark, DE 19716-3140, USA

Accepted 15 August 2007

Abstract

Due to the avascular nature of articular cartilage, solute transport through its extracellular matrix is critical for the maintenance and the functioning of the tissue. What is more, diffusion of macromolecules may be affected by the microstructure of the extracellular matrix in both undeformed and deformed cartilage and experiments demonstrate diffusion anisotropy in the case of large solute. However, these phenomena have not received sufficient theoretical attention to date.

We hypothesize here that the diffusion anisotropy of macromolecules is brought about by the particular microstructure of the cartilage network. Based on this hypothesis, we then propose a mathematical model that correlates the diffusion coefficient tensor with the structural orientation tensor of the network. This model is shown to be successful in describing anisotropic diffusion of macromolecules in undeformed tissue and is capable of clarifying the effects of network reorientation as the tissue deforms under mechanical load. Additionally, our model explains the anomaly that at large strain, in a cylindrical plug under unconfined compression, solute diffusion in the radial direction increases with strain.

Our results indicate that in cartilage the degree of diffusion anisotropy is site specific, but depends also on the size of the diffusing molecule. Mechanical loading initiates and/or further exacerbates this anisotropy. At small deformation, solute diffusion is near isotropic in a tissue that is isotropic in its unstressed state, becoming anisotropic as loading progresses. Mechanical loading leads to an attenuation of solute diffusion in all directions when deformation is small. However, loading, if it is high enough, enhances solute transport in the direction perpendicular to the load line, instead of inhibiting it.

Keywords: Diffusion–convection; Anisotropy; Soft tissue; Deformation; Cartilage

1. Introduction

Articular cartilage is a structurally inhomogeneous, anisotropic soft tissue covering the load-bearing surfaces of diarthrodial joints (Hunziker, 1992; Mow and Ratcliffe, 1997). Mechanically, cartilage shows strong nonlinear and anisotropic characteristics (Wu and Herzog, 2002; Jurvelin et al., 2003; Wang et al., 2003; Huang et al., 2005; Lei and Szeri, 2006).

The inhomogeneous and anisotropic nature of cartilage influences not only its mechanical but also its transport properties. Leddy and Guilak (2003) investigated diffusive transport of 3–500 kDa dextrans in porcine articular cartilage. They observed that the diffusion coefficient varied throughout the thickness of the cartilage for all sizes of dextran; however, the severity of such variation was size dependent. Leddy et al. (2006) demonstrated significant anisotropic diffusion of macromolecules (500 kDa dextran) in the surface zone. During compression, the anisotropy of solute transport might be triggered or escalated due to the ever-changing inhomogeneity and anisotropy of the microstructure (Dunlop and Quinn, 2002; Leddy et al., 2006).

Although experimental results amply demonstrate anisotropy of diffusion of neutral solutes in cartilage, the causes of this anisotropy are largely unknown. The proteoglycan-water gel is generally believed to provide resistance to solute transport in cartilage primarily through its fine porous structure (Maroudas, 1970, 1976; Torzilli

*Corresponding author. Tel.: +1 302 831 2008; fax: +1 302 831 3619.
E-mail address: szeri@me.udel.edu (A.Z. Szeri).

0021-9290/$ - see front matter © 2007 Elsevier Ltd. All rights reserved.
doi:10.1016/j.jbiomech.2007.08.005

et al., 1997; Nimer et al., 2003). Solute transport in cartilage is also found to be size dependent (Roberts et al., 1996; Nimer et al., 2003).

Even though proteoglycan content is an important factor in determining solute transport, the proteoglycan molecules require a stabilizing solid matrix to exert their full transport-limiting effect. Aggrecan proteoglycans attached to a hyaluron backbone are entangled with collagen fibers (Mow and Ratcliffe, 1997). The highly cross-linked collagen network immobilizes the glycosaminoglycans (GAGs). Netti et al. (2000) stated that GAG concentration is not the only factor that accounts for the resistance to macromolecule transport in soft tissues. They proposed that the collagen also affects macromolecule transport by binding and stabilizing the GAG components. That is, the collagen–proteoglycan bonds are identified as the main culprit in restricting solute mobility. Leddy et al. (2006) also hypothesized that anisotropy of diffusion is size dependent and is related to the collagen structure.

Theoretically, Han and Herzfeld (1993) studied the hindrance on the self or tracer diffusion of macromolecules in concentrated solutions and found that both aggregation and alignment of the background protein attenuated hindrance of globular protein. However, anisotropy of solute diffusion due to the microstructure of cartilage and compression of the tissue has not been fully explained. Previous theoretical studies on solute transport in cartilage (Mauck et al., 2003; Ferguson et al., 2004; Zhang and Szeri, 2005), viewed the tissue as an isotropic material.

Our hypothesis is that (i) resistance to solute diffusion in cartilage results from a reduction of the cross-sectional area available to the solute due to the presence of the solid matrix, and (ii) this reduction of pore cross section is modulated by the geometry of the collagen and GAG networks. The proteoglycan network is immobilized with the collagen network (Tepic et al., 1983). We will find it beneficial to borrow from Tepic et al. (1983) and study the influence of the collagen and GAG networks by investigating the influence of a single, 'equivalent network'.

The present study attempts to build a general model that correlates the diffusion coefficient tensor with the cartilage network orientation tensor. The model also describes collagen and GAG reorientation and the corresponding variation of the diffusion coefficient tensor as the tissue is mechanically loaded. By combining the diffusion coefficient tensor with the governing equations of Zhang and Szeri (2005, 2007), we investigate the effect of both inherent and loading-induced microstructure anisotropy on solute diffusion.

2. Methods

2.1. Governing equations

We envisage the tissue as a mixture of three intrinsically incompressible phases, an inviscid fluid (superscript w), a neutral solute (superscript f) and a hyperelastic, porous, solid matrix (superscript s), with a collagen fiber network (superscript c) embedded in the matrix. It is assumed, therefore, that the mechanical behavior of the tissue can be characterized by the conservation equations of mixture theory (Atkin and Craine, 1976; Bowen, 1980; Mow et al., 1980; Rajagopal and Tao, 1995).

2.1.1. Balance laws

Neglecting inertia and body force, the linear momentum equation for the mixture can be expressed as

$$\operatorname{div} \boldsymbol{T} = 0, \tag{1}$$

where $\boldsymbol{T}$ is the Cauchy stress of the mixture.

The collagen and GAG networks strongly influence the mechanical properties of the tissue. The charged, interdigitated GAG molecules resist compression; their contribution to the mechanical properties of the tissue is reflected in the compressive properties of solid matrix. The tensile properties of the tissue, on the other hand, are characterized by the stress–strain conditions in the collagen fibrils. The total stress of the mixture consists of the stress in the fluid $\boldsymbol{T}^{\mathrm{w}}$, the solute stress $\boldsymbol{T}^{\mathrm{f}}$, the matrix stress $\boldsymbol{T}^{\mathrm{s}}$, and the fiber stress $\boldsymbol{T}^{\mathrm{c}}$ (Section A, Supplement):

$$\boldsymbol{T} = \boldsymbol{T}^{\mathrm{s}} + \boldsymbol{T}^{\mathrm{w}} + \boldsymbol{T}^{\mathrm{f}} + \boldsymbol{T}^{\mathrm{c}}. \tag{2}$$

We hypothesize that the collagen and GAG networks influence not only the mechanical properties of the tissue but also its transport properties, as will be discussed in the sequel.

The balance of linear momentum for water makes use of Darcy's law

$$\phi^{\mathrm{w}}(\boldsymbol{v}^{\mathrm{w}} - \boldsymbol{v}^{\mathrm{s}}) = -\boldsymbol{k} \operatorname{grad} p, \tag{3}$$

where $\boldsymbol{v}^{\mathrm{w}}, \boldsymbol{v}^{\mathrm{s}}$ are velocity of fluid and solid, respectively and $\boldsymbol{k}$ is the permeability tensor.

Anisotropic permeability was observed in statically loaded middle zone cartilage explant by using both direct (Reynaud and Quinn, 2006) and indirect (Jurvelin et al., 2003) measurements. Soltz and Ateshian (2000) found the radial permeability to differ from axial permeability in the surface zone. They suggested that the difference was due to microstructure organization. Quinn et al. (2001) established a theoretical model for compression-induced anisotropic permeability. As the computations carried out in this study are for statically loaded cartilage, the expression of permeability will not alter solute concentration. However, we do account for the change in porosity with stress through Eq. (8).

In computations performed under dynamic conditions (Zhang and Szeri, 2007), we assumed isotropy. The permeability k, then a scalar, changed with porosity and, indirectly, with strain, according to

$$k = k_0 \exp\left[M\left(\frac{\phi^{\mathrm{w}} - \phi_0^{\mathrm{w}}}{1 - \phi^{\mathrm{w}}}\right)\right]. \tag{4}$$

Lai and Mow (1980) derived this constitutive equation for permeability from one-dimensional experiments. Here ϕ_0^{w} is the volume fraction of the interstitial fluid in the undeformed tissue.

Eqs. (3) and (4) are part of our diffusion/convection model that is proposed under both static and dynamic conditions. However, the computations we report on in the present paper are for statically strained cartilage only. Under equilibrium conditions there is no fluid flow; thus Eqs. (3) and (4) are not utilized and the poroelasticity of cartilage becomes irrelevant within the context of the present computations.

The solute diffusion equation is adopted from Zhang and Szeri (2005),

$$\frac{\partial c}{\partial t} + \boldsymbol{v}^{\mathrm{w}} \cdot \operatorname{grad} c = \frac{1}{\phi^{\mathrm{w}}} \operatorname{div}(\phi^{\mathrm{w}} \boldsymbol{D} \cdot \operatorname{grad} c). \tag{5}$$

Here $\boldsymbol{D}$ is the diffusivity (coefficient) tensor and c is the solvent-volume-based solute concentration, in correspondence with Quinn's experiments.

2.1.2. Diffusivity tensor

Let D_{a} represent the diffusion coefficient in the unobstructed solvent. We hypothesize that the diffusivity tensor consists of two components, both depending on the strain field of the extracellular matrix,

$$\boldsymbol{D} = D_{\mathrm{a}}[f_1(\phi^{\mathrm{w}})\boldsymbol{I} + f_2(\boldsymbol{\omega})]. \tag{6}$$

The first component results from the increase in diffusion-channel tortuosity owing to the presence of the solid matrix, and is dependent on local strain via the volume fraction through Eqs. (7) and (8). In contrast, the second component reflects the state of isotropy of the cartilage network through the network orientation tensor, $\boldsymbol{\omega}$, as determined by the fiber orientation distribution and the strain field, Eq. (10). The first component is isotropic; however, neither the second component of the diffusion tensor nor the diffusion tensor itself can be isotropic in a strained (other than uniformly dilatated) cartilage. The additional requirement for the isotropy of the second term is a constant value of the orientation distribution function (see Eq. (S8) of Supplement).

We adopt the Cohen–Turnbull–Yasuda model (Cohen and Turnbull, 1959; Yasuda et al., 1968) to correlate the decrease in the diffusion with an increase in tortuosity owing to the presence of the matrix. Therefore,

$$f_1(\phi^{\mathrm{w}}) = \exp\left[K_{\mathrm{f}}\left(1-\frac{1}{\phi^{\mathrm{w}}}\right)\right], \tag{7}$$

where K_{f} is a constant that is dependent on solute size.

We chose the Cohen–Turnbull–Yasuda model because it makes solute diffusion dependent on both the water content of the tissue and the size of the solute. As the coefficient K_{f} is proportional to solute size, diffusion of the large solute is restricted by compression to a greater extent than that of the small solute. This phenomenon has been demonstrated in the experiments of Quinn et al. (2001, 2002), and Nimer et al. (2003). Our previous study (Zhang and Szeri, 2005) compared the predictions of the Cohen–Turnbull–Yasuda model with the Mackie and Mears model (Mackie and Mears, 1955) and decided in favor of the former.

The porosity of the tissue also changes during deformation (Zhang and Szeri, 2005), thus in (7) we substitute

$$\phi^{\mathrm{w}} = 1-(1-\phi_0^{\mathrm{w}})\det \boldsymbol{C}^{-1/2}. \tag{8}$$

We hypothesized earlier that both collagen and GAG networks contribute to diffusion anisotropy. However, since the GAG network is immobilized by the collagen network, we made f_2 in Eq. (6) to be a function of a single 'equivalent network' orientation tensor, the latter depicting the changing geometry of both collagen and GAG networks as the cartilage is deforming. For expediency, and because no relevant data is known to us, we assume a simple power dependence for this relationship in the form

$$f_2(\boldsymbol{\omega}) = c_1(\boldsymbol{\omega})^{c_2}, \tag{9}$$

where $c_1(\phi^{\mathrm{w}}) \geqslant 0$, $c_1 \to 0$ as $\phi^{\mathrm{w}} \to 1$, is a coefficient weighting the importance of fiber network anisotropy. The fact that the water content of the cartilage depends on strain through Eq. (8), makes c_1 vary from point to point in the mechanically strained cartilage. We have no local data on anisotropic diffusion available to us and, therefore, in the computations we estimate a representative (effective) value $\bar{c}_1 = \text{const}$ for given orientation distribution function. The exponent c_2 defines 'sensitivity to anisotropy' by simulating the experimental data of Leddy et al. (2006); we found it to depend on the density of fiber packing and on the size of the solute (Figs. 1 and 3). Experimental data is needed, however, to investigate the validity of Eq. (9) and the exact representations of c_1 and c_2.

To evaluate the diffusivity tensor (6) of the solute in the undeformed as well as in the deformed tissue, it will be necessary to establish a model for fiber orientation. This is attempted in Section B of Supplement.

The basic units of collagen are the rod-like tropocollagen molecules, polymerized into larger collagen fibrils (Clarke, 1971; Eyer, 1980; Mow et al., 1989). GAGs are also rod-like and are linked at one end to the proteoglycan core protein (Muir, 1977; Heinegard and Paulsson, 1984; Quinn et al., 2001). Here we apply the composite cylinder model (Ault and Hoffman, 1992; Schwartz et al., 1994; Lei and Szeri, 2006) to describe the orientation of the equivalent cartilage network.

We make the following assumptions: (1) the cartilage fibril is locally straight and can only support tensile stress, (2) there is no slip between fibril and matrix, (3) fibril with fibril interaction is negligible (Section B, Supplement).

We represent fibril configuration by the 'fibril orientation tensor' which, in the deformed state, has the form (see Section B, Supplement)

$$\boldsymbol{\omega} = \iint \frac{3}{|\boldsymbol{FN}|^2}\boldsymbol{FN}\otimes\boldsymbol{FN}\Psi(\Theta,\Phi)\sin\Theta\,\mathrm{d}\Theta\,\mathrm{d}\Phi. \tag{10}$$

Note that $\boldsymbol{\omega} \propto \boldsymbol{I}$ only when $\Psi(\Theta,\Phi) = \text{const}$ (isotropic distribution) and $\boldsymbol{F} \propto \boldsymbol{I}$. If there is deformation other than uniform dilatation, the orientation tensor remains a general tensor even if the initial orientation distribution function is a constant. The factor 3 in Eq. (10) renders $\boldsymbol{\omega} = \boldsymbol{I}$ when the fibrils are isotropically distributed and the tissue is undeformed.

Introducing Eq. (8) into (7) and (10) into (9), respectively, and substituting into Eq. (6), we obtain the diffusion coefficient tensor in the deformed cartilage tissue

$$\boldsymbol{D} = D_{\mathrm{a}}\left\{\exp\left(K_{\mathrm{f}}\left[\frac{(\phi_0^{\mathrm{w}}-1)detC^{-1/2}}{1-(1-\phi_0^{\mathrm{w}})\det C^{-1/2}}\right]\right)\boldsymbol{I} + \left[c_1\left(\iint\frac{3}{|\boldsymbol{FN}|^2}\boldsymbol{FN}\otimes\boldsymbol{FN}\Psi(\Theta,\Phi)\sin\Theta\,\mathrm{d}\Theta\,\mathrm{d}\Phi\right)^{c_2}\right]\right\}. \tag{11}$$

Here $\boldsymbol{N}$ is the initial fiber direction, $\Psi(\Theta,\Phi)$ is the initial orientation distribution function, $\boldsymbol{F}$ is the deformation gradient and (Θ,Φ) are angular coordinates.

The orientation distribution functions Ψ_{H}, Ψ_{R}, and Ψ_{V}, we employed for the surface, the middle and the deep zones, respectively, are taken from Lei and Szeri (2006). The reasoning there is that in first approximation the collagen fibers are mostly aligned to the surface in the surface zone (Minns and Steven, 1977), in the middle zone they are randomly distributed (Weiss et al., 1968), while they are dominantly perpendicular to the cartilage–bone interface in the deep zone (Aspden and Hukins, 1981; Clark, 1991). The orientation distribution functions are independent of water content of the tissue.

2.2. Constitutive equations

There have been numerous macroscopic constitutive models proposed over the past decade for the mechanical properties of cartilage (Mow et al., 1980; Holmes and Mow, 1990; Cohen et al., 1998; Oloyede and Broom, 1991; Soltz and Ateshian, 2000; Nguyen and Oloyede, 2001). Researchers currently are attempting to develop microstructural models for this purpose (Soulhat et al., 1999; Li et al., 1999, 2005; Wilson et al., 2004). Lei and Szeri (2007c) developed a comprehensive microstructural model to account for poroelasticity, tension–compression nonlinearity, inhomogeneity, intrinsic viscoelasticity, and anisotropy. Here, we base our constitutive model on the microstructural model of Lei and Szeri (2006). This model uses distribution functions to describe the geometric orientation of the collagen fibrils, making it readily adaptable to different types of fibril configurations. We also make use of the hyperfoam strain energy function (Hill, 1978; Lei and Szeri, 2007b).

2.2.1. Solid matrix

The hyperfoam strain energy function (Hill, 1978; Storakers, 1986) is

$$\boldsymbol{W} = \frac{2\mu}{\alpha^2}\left[\lambda_1^{\alpha}+\lambda_2^{\alpha}+\lambda_3^{\alpha}-3+\frac{1}{\beta}(J^{-\alpha\beta}-1)\right], \tag{12}$$

where λ_1, λ_2, λ_3 are the principal stretches, $J = \det \boldsymbol{F}$ is the ratio of deformed to original volume at a point, while the constants μ, α and β relate to the initial aggregate modulus and Poisson's ratio through

$$H_{\mathrm{A0}} = 2(\beta+1)\mu,\ \nu_{\mathrm{s}} = \frac{\beta}{1+2\beta}. \tag{13}$$

The constants α and β define the nonlinearity of the material.

2.2.2. Fibril network

If σ represents the effective elastic stress in the fiber of orientation $\boldsymbol{n}$, then single-fibril stress in the global coordinate system x_{i} is given by

$$\tilde{\boldsymbol{T}}_{\mathrm{E}}^{\mathrm{c}} = \sigma\boldsymbol{n}\otimes\boldsymbol{n}. \tag{14}$$

The effective stress of the fibril network can be obtained by weighting the single-fiber stress with the orientation distribution function (Chou, 1992) and summing over the regions in which the fibers are in tension (Lei and Szeri, 2006)

$$\boldsymbol{T}_{\mathrm{E}}^{\mathrm{c}} = \int_0^{2\pi} \int_{G(\Phi)}^{H(\Phi)} \hat{T}_{\mathrm{E}}^{\mathrm{c}} \Psi(\Theta, \Phi) \sin\Theta \, \mathrm{d}\Theta \, \mathrm{d}\Phi. \tag{15}$$

Here $H(\Phi)$, $G(\Phi)$ represent the boundaries of the region in tension relative to the initial configuration.

The one-dimensional fibril stress σ is assumed to depend nonlinearly on fibril strain as (Li et al., 1999)

$$\sigma = \left(E_{c_0} + \frac{1}{2} E_{c_1} \varepsilon_c\right) \varepsilon_c. \tag{16}$$

Here ε_c is the fibril's tensile strain and E_{c_0} and E_{c_1} are constants.

Substituting Eqs. (14) and (16) into Eq. (15), we obtain the stress for the fibril network

$$\boldsymbol{T}_{\mathrm{E}}^{\mathrm{c}} = \int_0^{2\pi} \int_{G(\Phi)}^{H(\Phi)} \boldsymbol{FN} \otimes \boldsymbol{FN} \left(E_{c_0} + \frac{1}{2} E_{c_1} \varepsilon_c\right) \times \varepsilon_c \Psi(\Theta, \Phi) \sin\Theta \, \mathrm{d}\Theta \, \mathrm{d}\Phi \tag{17}$$

In summary, Eqs. (1), (S4), (3), (5), (11), (12) and (17) compose our model for neutral-solute transport in cartilage with microstructure.

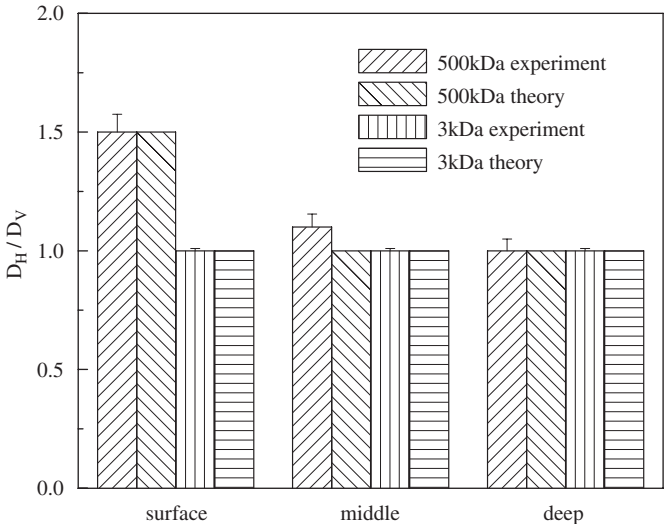

Fig. 1. Ratio of diffusion coefficients parallel and perpendicular to the primary fiber direction (experiment Leddy et al., 2006).

3. Discussion of results

We implement the formulation in the finite element code ABAQUS. Axisymmetric elements CAX4P and CAX4 are used to model the solid matrix and the fiber network, respectively. The two elements share the nodes. Soil consolidation procedure is employed to solve Eq. (1), and heat transfer procedure to solve Eq. (5). The parameters needed to simulate solute diffusion in cartilage, including microstructural effects, are μ, α, β, k, Ψ, E_{c_0}, E_{c_1}, ϕ_0; D_0, K_{f}, c_1, c_1. No experimental data are available to estimate all parameters; thus the value or range of some must be assumed.

We examine the validity of our model by comparing its predictions with experimental data for neutral-solute diffusion in both undeformed and deformed cartilage tissue. We perform two simulations (see Section C of Supplement)

3.1. Diffusion in unloaded tissue

A considerable number of unidirectional measurements of solute diffusion in undeformed cartilage have been reported in the literature (Maroudas, 1971, 1976; Allhands et al., 1984; Schneiderman et al., 1995; Roberts et al., 1996). However, only scant attention has been paid to multi-dimensional diffusion or to diffusion anisotropy. Leddy et al. (2006) discussed experiments on full thickness (all three zones) cartilage explants from femoral porcine condyles. In these experiments, the explants were soaked in concentrated solutions of 3 or 500 kDa dextrans for a period of 3 days prior to the diffusion tests.

To illustrate the performance of our model, we first compare its predictions with data from Leddy et al. (2006) in Fig. 1. For the computations the unstrained diffusion coefficient of the 500 kDa dextran in the surface zone of the cartilage, $D_{0z} = 12\,\mu\mathrm{m}^2/\mathrm{s}$, was taken from Leddy and Guilak (2003). Leddy demonstrated the anisotropy she had observed by displaying the mean ratio of diffusion coefficients parallel and perpendicular to the primary fiber direction. Though very useful, this information is insufficient for us to estimate all parameters in the model and need to assume some. We guess fiber orientation s.d. (standard deviation) $\sigma_{\mathrm{c}} = 0.5$ and tissue porosity $\phi_0^{\mathrm{w}} = 0.8$. Other parameters, obtained through curve-fitting (Lei and Szeri, 2007a) to the 500 kDa data, are $K_{\mathrm{f}} = 17.3$, $c_1 = 0.000141$ and $c_2 = 16.5$, 13.8 and 2.3, respectively, in the surface, middle, and deep zone of the cartilage. The value of c_2 changes as expected. As the transport medium changes from the surface to the deep zone, we expect c_2 to vary with depth as fiber density varies throughout the thickness of the tissue (Comper, 1991). Moreover, collagen fibers in the deep zone are widely spaced compared with the surface zone (Hwang et al., 1992; Jeffery et al., 1991), leading to a lesser effect on the diffusion coefficient here compared to the other two zones. Therefore, c_2 in the deep zone is expected to be smaller than it is for the surface zone. For diffusing the 3 kDa dextran, the model parameters are $K_{\mathrm{f}} = 7.1$, $c_1 = 0.000141$ and $c_2 = 5.6$, 4.2 or 2.1 respectively, in the surface, middle, and deep zone of the cartilage.

Solute diffusion can be significantly affected by the fiber network configuration. Fig. 2 shows the ratio of radial diffusivity to axial diffusivity versus fiber orientation s.d. for 3 and 500 kDa dextran in cartilage with horizontally distributed fiber network. Three kilodaltones dextran diffusion is not affected by the variation of fiber network configuration, whereas 500 kDa dextran is greatly influenced by the fiber orientation s.d. As σ is varied from 0.1 to 1.5, i.e. the geometry changed from a horizontally organized to a more random network, the anisotropy diminishes.

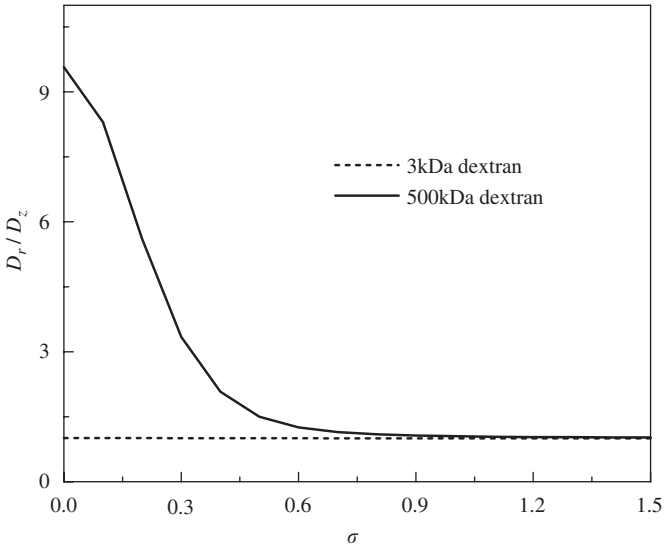

Fig. 2. Diffusion coefficient ratio versus fiber orientation s.d.

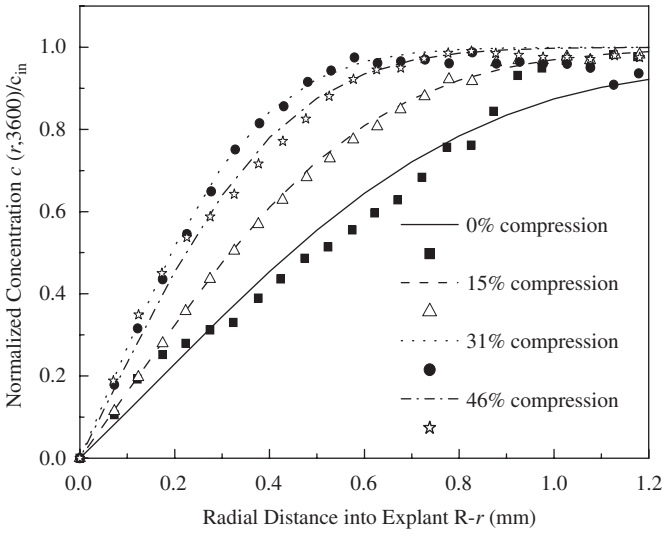

Fig. 3. Concentration distribution of 40 kDa dextran, static loading. (symbols: Quinn et al., 2002; curves: theory).

3.2. Diffusion in deformed tissue

To further demonstrate the feasibility of the current model, we compare its predictions to data under static loading (Quinn et al., 2002) in Fig. 3. Quinn et al. (2002) carried out their experiment within the middle zone of the cartilage, where we assumed random fiber orientation. As in the previous study (Zhang and Szeri, 2005), the diffusion coefficient at zero compression, $D_0 = 40\,\mu m^2/s$ for 40 kDa dextran, was obtained by fitting Quinn's analytical solution to his own experimental data. We assumed the fiber constants $E_{c_0} = 10$ MPa, $E_{c_1} = 2000$ MPa, and the porosity $\phi_0^w = 0.8$. The other parameters were acquired by fitting (Lei and Szeri, 2007a) to concentration distribution data at 15%, 31% and 46% static compression: $H_{A0} = 0.78$ MPa, $\alpha = 1.18$, $v_s = 0.41$, $k = 8.5e{-}15\,m^4/N\,s$, $K_f = 16.75$, $c_1 = 0.00018$ and $c_2 = 14.3$.

Tissue properties vary greatly among different cartilage explants. Our parameters were obtained by curve fitting to actual experimental data and fall within the data ranges we examined (Table 1). Lei and Szeri (2006) investigated the variation of Poisson's ratio with fiber orientation. They examined four orientation distribution functions: random, vertical, horizontal and orthogonal (Soulhat et al., 1999). Under tensile loading when the Poisson's ratio of the matrix is set at 0.3, they report $0.4 > v_{12} > 1.2$, depending on fiber orientation.

At small-to-medium strain, the data show the diffusion coefficient in the radial direction gradually decreasing with strain (Fig. 4). At large strain, however, this tendency is reversed, the radial diffusion coefficient increases with increasing strain. This phenomenon can be explained with the aid of Eq. (11). Two factors regulate solute transport in cartilage under mechanical compression; one is the increase of path length due to loss of water; the other is the variation of pathway due to the deformation of cartilage network geometry. The cartilage fibers will be realigned and eventually stretched if the deformation is sufficiently large (Mow and Guo, 2002). For small solute, a change in

Table 1
Predicted aggregate modulus, Poisson's ratio and permeability for Quinn's experiment

Aggregate modulus H_{A0} (MPa)	0.78	0.894 ± 0.293[a] 0.4–0.9[b]
Poisson's ratio, v_S	0.41	0.396 ± 0.023[a] 0.13–0.45[b] 0.30–0.42[c]
Permeability, k ($\times 10^{-15}\,m^4/N\,s$)	8.5	9.8 ± 3.9[d]

[a]Athanasiou et al. (1991).
[b]Mow and Guo (2002).
[c]Li et al. (2003).
[d]Huang et al. (2005).

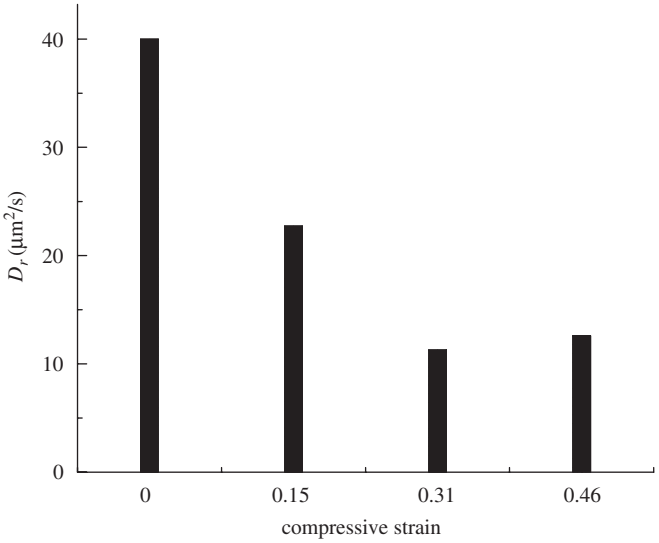

Fig. 4. Effect of compressive strain on radial diffusivity.

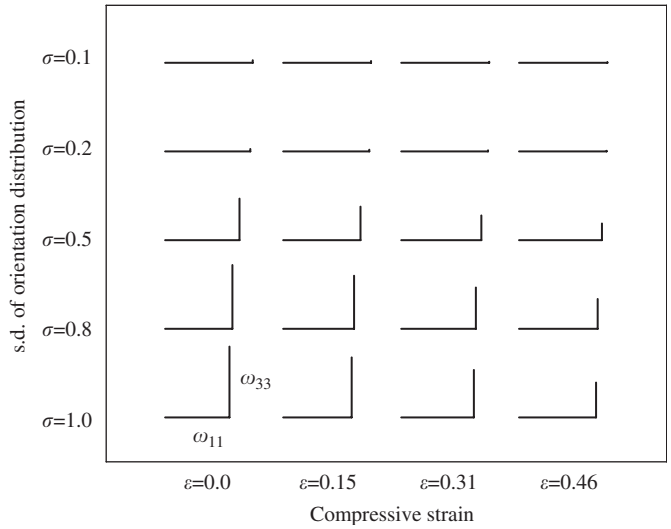

Fig. 5. Change of fiber orientation with compressive strain (horizontal orientation distribution, Ψ_H).

cartilage network geometry will not influence diffusion. Diffusion of the large solute, however, will favor the direction perpendicular to compression, owing to the decrease in tortuosity in that direction. The two factors regulating solute transport in cartilage compete with one another during loading process. The first factor is dominant at small strain while beyond a certain degree of static compression, the second factor will dominate and here diffusion of the large solute will be enhanced.

Fig. 5 illustrates the change of fiber orientation with strain for horizontally distributed fibers. The length of a line segment in this figure is proportional to the relative strength of orientation in the direction of that line segment. When $\sigma \to 0$, $\omega_{33} \to 0$ and all fibers are likely to be directed along the horizontal. When $\sigma \to \infty$, $\omega_{33} \to \omega_{11}$; thus the horizontal and vertical directions are equally favored. Note that here the off-diagonal terms vanish, $\omega_{22} \to \omega_{11}$ and $\omega_{11} + \omega_{22} + \omega_{33} = 1$. We compute fiber reorientation under unconfined compression. The sample utilized in these computations has radius 1.4 mm and thickness 0.2 mm. The mechanical properties of the tissue adopted are as follows: $H_A = 0.35$ MPa, $v_s = 0.38$, $\alpha = 0.87$, $E_{c_0} = 16$ MPa, $E_{c_1} = 5000$ MPa, $K_f = 16.75$, $c_1 = 0.00018$, $c_2 = 14.3$. The result is in qualitative agreement with those of Alhadlaq and Xia (2004). We carried out the computation only for horizontally distributed fiber configuration since the effect of microstructure on solute diffusion is greatest in the surface zone of the cartilage (Leddy et al., 2006).

Conflict of interest

We performed this research under Grant no. P20RR16458 from the National Center for Research Resources (NCRR), a component of the National Institutes of Health (NIH). Its contents are solely our responsibility and do not necessarily represent the official views of NCRR or NIH. We had no other funding for this research.

Acknowledgements

Grant no. P20RR16458 from the National Center for Research Resources (NCRR), a component of the National Institutes of Health (NIH) made this publication possible. Its contents are solely the responsibility of the authors and do not necessarily represent the official views of NCRR or NIH. We are grateful to Dr. Fulin Lei of the University of Delaware for his user-defined ABAQUS subroutine matmicronl.obj, and for his valuable advice.

Appendix A. Supporting Information

Supplementary data associated with this article can be found in the online version at doi:10.1016/j.jbiomech.2007.08.005.

References

Alhadlaq, H.A., Xia, Y., 2004. The structural adaptations in compressed articular cartilage by microscopic MRI (mMRI) T2 anisotropy. Osteoarthritis and Cartilage 12 (11), 887–894.

Allhands, R.V., Torzilli, P.A., Kallfelz, F.A., 1984. Measurement of diffusion of uncharged molecules in articular-cartilage. Cornell Veterinarian 74 (2), 111–123.

Aspden, R.M., Hukins, D.W.L., 1981. Collagen organization in articular cartilage, determined by X-ray diffraction, and its relationship to tissue function. Proceedings of the Royal Society B 212, 299–304.

Athanasiou, K.A., Rosenwasser, M.P., Buckwalter, J.A., Malinin, T.I., Mow, V.C., 1991. Interspecies comparisons of in situ intrinsic mechanical properties of distal femoral cartilage. Journal of Orthopaedic Research 9 (3), 330–340.

Atkin, R.J., Craine, R.E., 1976. Continuum theories of mixtures: basic theory and historical development. Quarterly Journal of Mechanics and Applied Mathematics XXIX, 209–244.

Ault, H.K., Hoffman, A.H., 1992. A composite micromechanical model for connective tissues: part I—Theory. Journal of Biomechanical Engineering 114, 137–141.

Bowen, R.M., 1980. Incompressible porous media models by use of the theory of mixtures. International Journal of Engineering Science 18, 1129–1148.

Chou, T.W., 1992. Microstructural Design of Fiber Composites. Cambridge University Press, Cambridge.

Clark, J.M., 1991. Variation of collagen fiber alignment in a joint surface—a scanning electron microscope study of the tibial plateau in dog, rabbit, and man. Journal of Orthopaedic Research 9, 246–257.

Clarke, I.C., 1971. Articular cartilage: a review and scanning electron microscope study. I. The interterritorial fibrillar architecture. Journal of Bone and Joint Surgery 53B, 732.

Cohen, M.R., Turnbull, D., 1959. Molecular transport in liquids and glasses. Journal of Chemical Physics 31, 1164–1169.

Cohen, B., Lai, W.M., Mow, V.C., 1998. A transversely isotropic biphasic model for unconfined compression of growth plate and chondroepiphysis. Journal of Biomechanical Engineering 120, 491–496.

Comper, W.D., 1991. Physicochemical aspects of cartilage extracellular matrix. In: Hall, B., Newman, S. (Eds.), Cartilage, Molecular Aspects. CRC Press, Boston, pp. 59–96.

Dunlop, A.E., Quinn, T.M., 2002. Development of a method for measurement of anisotropic and inhomogeneous solute diffusion in

compressed cartilage. European Cells and Materials 4 (Suppl. 1), 48–49.
Eyer, D.R., 1980. Collagen: molecular diversity in the body's protein scaffold. Science 207, 1315.
Ferguson, S.J., Ito, K., Nolte, L.P., 2004. Fluid flow and convective transport of solutes within the intervertebral disc. Journal of Biomechanics 37, 213–221.
Han, J., Herzfeld, J., 1993. Macromolecular diffusion in crowded solutions. Biophysics Journal 65, 1155–1161.
Heinegard, D., Paulsson, M., 1984. Structure and metabolism of proteoglycans. In: Piez, K.A., Reddi, A.H. (Eds.), Extracellular Matrix Biochemistry, pp. 277–328.
Hill, R., 1978. Aspects of invariance in solid mechanics. Advances in Applied Mechanics 18, 1–75.
Holmes, M.H., Mow, V.C., 1990. The Nonlinear characteristics of soft gels and hydrated connective tissues in ultrafiltration. Journal of Biomechanics 23 (11), 1145–1156.
Huang, C.Y., Stankiewicz, A., Ateshian, G.A., Mow, V.C., 2005. Anisotropy, inhomogeneity, and tension–compression nonlinearity of human glenohumeral cartilage in finite deformation. Journal of Biomechanics 38, 799–809.
Hunziker, E.B., 1992. Articular cartilage structure in humans and experimental animals. In: Kuettner, K., et al. (Eds.), Articular Cartilage and Osteoarthritis. Raven Press, New York, pp. 183–199.
Hwang, W.S., Li, B., Jin, L.H., Ngo, K., Schachar, N.S., Hughes, G.N., 1992. Collagen fibril structure of normal, aging, and osteoarthritic cartilage. Journal of Pathology 167, 425–433.
Jeffery, A.K., Blunn, G.W., Archer, C.W., Bentley, G., 1991. Three-dimensional collagen architecture in bovine articular cartilage. Journal of Bone and Joint Surgery - British Volume 73-B (5), 795–801.
Jurvelin, J.S., Buschmann, M.D., Hunziker, E.B., 2003. Mechanical anisotropy of the human knee articular cartilage in compression. Proceedings of the Institution of Mechanical Engineers Part H 217, 215–219.
Lai, W.M., Mow, V.C., 1980. Drag-induced compression of articular cartilage during a per-meation experiment. Biorheology 17, 111–123.
Leddy, H.A., Guilak, F., 2003. Site-specific molecular diffusion in articular cartilage measured using fluorescent recovery after photo bleaching. Annals of Biomedical Engineering 31, 753–760.
Leddy, H.A., Haider, M.A., Guilak, F., 2006. Diffusional anisotropy in collagenous tissues: fluorescence imaging of continuous point photobleaching. Biophysics Journal 91, 311–316.
Lei, F.L., Szeri, A.Z., 2006. The influence of fibril organization on the mechanical behaviour of articular cartilage. Proceedings of the Royal Society A 462, 3301–3322.
Lei, F.L., Szeri, A.Z., 2007a. Inverse analysis of constitutive models: biological soft tissues. Journal of Biomechanics 40 (4), 936–940.
Lei, F.L., Szeri, A.Z., 2007b. A study of large deformation of articular cartilage with a fibril-reinforced poroelastic model, IASTED International Conference on Biomedical Engineering, Innsbruck, Paper No. 555-008.
Lei, F.L., Szeri, A.Z., 2007c. Predicting articular cartilage behavior with a non-linear microstructural model. The Open Mechanics Journal 1, 1–10.
Li, L.P., Soulhat, J., Buschmann, M.D., Shirazi-Adl, A., 1999. Nonlinear analysis of cartilage in unconfined ramp compression using a fibril reinforced poroelastic model. Clinical Biomechanics 14, 673–682.
Li, L.P., Buschmann, M.D., Shirazi-Adl, A., 2003. Strain-rate dependent stiffness of articular cartilage in unconfined compression. Journal of Biomechanical Engineering 125, 161–168.
Li, L.P., Herzog, W., Korhonen, R.K., Jurvelin, J.S., 2005. The role of viscoelasticity of collagen fibers in articular cartilage: axial tension versus compression. Medical Engineering and Physics 27, 51–57.
Mackie, J.S., Mears, P., 1955. The diffusion of electrolytes in a cation exchange resin membrane. I. Theoretical. Proceedings of the Royal Society A 232, 498–509.
Maroudas, A., 1970. Distribution and diffusion of solutes in articular cartilage. Biophysics Journal 10, 365–379.
Maroudas, A., 1976. Transport of solutes through cartilage: permeability to large molecules. Journal of Anatomy 122 (2), 335–347.
Mauck, R.L., Hung, C.T., Ateshian, G.A., 2003. Modeling of neutral solute transport in a dynamically loaded porous permeable gel: implications for articular cartilage biosynthesis and tissue engineering. Journal of Biomechaical Engineering 125, 602–614.
Minns, R., Steven, F., 1977. The collagen fibril organization in human articular cartilage. Journal of Anatomy 123, 437–457.
Mow, V.C., Guo, X.E., 2002. Mechano-electrochemical properties of articular cartilage: their inhomogeneities and anisotropies. Annual Review of Biomedical Engineering 4, 175–209.
Mow, V.C., Ratcliffe, A., 1997. Structure and function of articular cartilage and meniscus. In: Mow, V.C., Hayes, W.C. (Eds.), Basic Orthopaedic Biomechanics. Lippincott Raven Publishers, Philadelphia, pp. 113–177.
Mow, V.C., Kuei, S.C., Lai, W.M., Armstrong, C.G., 1980. Biphasic creep and stress-relaxation of articular cartilage in compression theory and experiments. Journal of Biomechanical Engineering Transactions ASME 102 (1), 73–84.
Mow, V.C., Proctor, C.S., Kelly, M.A., 1989. Biomechanics of articular cartilage. In: Nordin, M.A., Frankel, V.H. (Eds.), Basic Biomechanics of the Muskuloskeletal System, second ed. Lea and Febiger Publishers, Philadelphia.
Muir, H., 1977. Molecular approach to the understanding of osteoarthritis. Annals of Rheumatic Diseases 36 (3), 199–208.
Netti, P.A., Berk, D.A., Swartz, M.A., Grodzinsky, A.J., Jain, R.K., 2000. Role of extracellular matrix assembly in interstitial transport in solid tumors. Cancer Research 60 (9), 2497–2503.
Nguyen, T., Oloyede, A., 2001. Predictive rheological models for the consolidation behaviour of articular cartilage under static loading. Proceedings of the Institute of Mechanical Engineers, H 215, 565–577.
Nimer, E., Schneiderman, R., Maroudas, A., 2003. Diffusion and partition of solutes in cartilage under static load. Biophysical Chemistry 106 (2), 125–146.
Oloyede, A., Broom, N.D., 1991. Is classical consolidation theory applicable to articular cartilage deformation? Clinical Biomechanics 6, 206–212.
Quinn, T.M., Dierickx, P., Grodzinsky, A.J., 2001. Glycosaminoglycan network geometry may contribute to anisotropic hydraulic permeability in cartilage under compression. Journal of Biomechanics 34, 1483–1490.
Quinn, T.M., Studer, C., Grodzinsky, A.J., Meister, J.J., 2002. Preservation and analysis of nonequilibrium solute concentration distributions within mechanically compressed cartilage explants. Journal of Biochemical and Biophysical Methods 52 (2), 83–95.
Rajagopal, K.R., Tao, L., 1995. Mechanics of Mixtures. World Scientific Publishing Co, London.
Reynaud, B., Quinn, T.M., 2006. Anisotropic hydraulic permeability in compressed articular cartilage. Journal of Biomechanics 39, 131–137.
Roberts, S., Urban, J.P., Evans, H., Eisenstein, S.M., 1996. Transport properties of the human cartilage endplate in relation to its composition and calcification. Spine 21, 415–420.
Schneiderman, R., Snir, E., Popper, O., Hiss, J., Stein, H., Maroudas, A., 1995. Insulin-like growth factor-I and its complexes in normal human articular cartilage: Studies of partition and diffusion. Archives In Biochemistry and Biophysics. 324 (1), 159–172.
Schwartz, M.H., Leo, P.H., Lewis, J.L., 1994. A microstructural model for the elastic response of articular cartilage. Journal of Biomechanics 27 (7), 865–873.
Soltz, M.A., Ateshian, G.A., 2000. A conewise linear elasticity mixture model for the analysis of tension-compression nonlinearity in articular cartilage. Journal of Biomechanical Engineering 122, 576–586.
Soulhat, J., Buschmann, M.D., Shirazi-Adl, A., 1999. A fibril-network-reinforced biphasic model of cartilage in unconfined compression. Journal of Biomechanical Engineering 121, 340–347.
Storakers, B., 1986. On material representation and constitutive branching in finite compressible elasticity. Journal of Mechanics and Physics of Solids. 34, 125–145.

Tepic, S., Macirowski, T., Mann, R.W., 1983. Mechanical-properties of articular-cartilage elucidated by osmotic loading and ultrasound. Proceedings of the National Academy of Science 80 (11), 3331–3333.

Torzilli, P.A., Arduino, J.M., Gregory, J.D., Bansal, M., 1997. Effect of proteoglycan removal on solute mobility in articular cartilage. Journal of Biomechanics 30 (9), 895–902.

Wang, C.C.B., Chahine, N.O., Hung, C.T., Ateshian, G.A., 2003. Optical determination of anisotropic material properties of bovine articular cartilage in compression. Journal of Biomechanics 36, 339–353.

Weiss, C., Rosenberg, L., Helfet, A.J., 1968. An ultrastructural study of normal young adult human cartilage. Journal of Bone and Joint Surgery 50A, 663–674.

Wilson, W., van Donkelaar, C.C., van Rietbergen, B., Ito, K., Huiskes, R., 2004. Stresses in the local collagen network of articular cartilage: a poroviscoelastic fibril-reinforced finite element study. Journal of Biomechanics 37, 357–366.

Wu, J.Z., Herzog, W., 2002. Elastic anisotropy of articular cartilage is associated with the microstructures of collagen fibers and chondrocytes. Journal of Biomechanics 35 (7), 931–942.

Yasuda, H., Lamaze, C.E., Ikenberry, L.D., 1968. Permeability of solutes through hydrated polymer membranes. Makromolekular Chemie 118, 19–35.

Zhang, L., Szeri, A.Z., 2005. Transport of neutral solute in articular cartilage: effects of loading and particle size. Proceedings of the Royal Society A 461, 2021–2042.

Zhang, L., Szeri, A.Z., 2007. Transportation of neutral solute in deformable, anisotropic soft tissue. Journal of Computational and Applied Mathematics 53, 232–243.

Further reading

Barocas, V.H., Tranquillo, R.T., 1997. An anisotropic biphasic theory of tissue-equivalent mechanics: the interplay among cell traction, fibrillar network deformation, fibril alignment, and cell contact guidance. Journal of Biomechanical Engineering 119 (2), 137–145.

Farquhar, T., Dawson, P.R., Torzilli, P.A., 1990. A microstructural model for the anisotropic drained stiffness of articular-cartilage. Journal of Biomechanical Engineering 112 (4), 414–425.

Schmid, T.M., Li, J., Muehleman, C., Wimmer, M., Irving, T.C., 2004. Cartilage compression changes collagen fiber orientation as measured by small angle X-ray diffraction. Transactions of the Orthopedic Research Society 29, 0230.

Spencer, A.J.M., 1972. Deformations of Fibre-Reinforced Materials. Oxford University Press, Oxford.